

SPATIOTEMPORAL MODELING OF ACID RAIN CHEMISTRY IN TROPICAL JAVA USING MIXED-EFFECTS MODELS: DEPOSITION PATTERNS AND THRESHOLD EXCEEDANCE

Rita Hidayati^{1,2}, Mochamad Aryono Adhi^{2*}, and Adi Mulsandi³

¹Agency for Meteorology Climatology and Geophysics, Jakarta 10720, Indonesia

²Physics Study Program, Universitas Negeri Semarang, Semarang 50229, Indonesia

³Meteorology Study Program, School of Meteorology, Climatology, and Geophysics (STMKG),
Tangerang Kota 15119, Indonesia

*E-mail: aryono_adhi@yahoo.com

Received: June 2, 2025

Reviewed: July 9, 2025

Accepted: October 10, 2025

ABSTRACT

Acid deposition in tropical regions remains under-characterized despite rapid urbanization and increasing emissions. This study examines the spatiotemporal variability of rainwater acidity across Java Island, Indonesia, based on five years (2019–2023) of event-based data from thirteen monitoring stations. Weekly measurements of pH, SO_4^{2-} , NO_3^- , NH_4^+ , Cl^- , and rainfall volume were analyzed using spatial mapping, seasonal stratification, and linear mixed-effects modeling. Results show that 47% of rain events exhibited $\text{pH} < 5.6$, while sulfate and nitrate exceeded critical ecological thresholds in up to 34% of cases, particularly during monsoon transitions. Ammonium buffering was observed but often insufficient in urban areas. Rainfall volume was significantly associated with ion concentrations, yet episodic deposition remained substantial even during high-precipitation periods. These findings highlight the dual role of tropical rainfall as both cleanser and vector of atmospheric pollutants. Our findings provide a scientific basis for incorporating acid deposition into Indonesia's environmental monitoring programs.

Keywords: Rainwater chemistry, Acid deposition, Spatiotemporal modeling, Mixed-effects model, Event-based monitoring, Java Island, Wet deposition, Monsoonal rainfall.

1. Introduction

Atmospheric deposition represents one of the most direct and consequential links between human activity and ecosystem vulnerability [1]–[6]. In tropical monsoon systems, this linkage is intensified by the coincidence of high atmospheric loading and abrupt convective precipitation, leading to chemically charged rainfall episodes with ecological implications. On Java Island, Indonesia's most industrialized and densely populated region, this linkage is particularly relevant due to the convergence of rapid urbanization, high fossil fuel consumption, and seasonal monsoonal dynamics. In tropical monsoon systems, the combination of high atmospheric loading and abrupt convective precipitation leads to chemically charged rainfall episodes with ecological implications. Rainwater, once perceived primarily as a benign cleansing agent of the atmosphere, has evolved into a chemically active vector carrying the residues of combustion, agriculture, and industrial processes [7]–[17]. In the global discourse on acid rain and nitrogen pollution, attention has long been centered on the Northern Hemisphere, where emission intensities and

environmental monitoring regimes are well-established [18]. Yet the tropics, especially fast-urbanizing regions under monsoonal regimes, are no longer peripheral to this phenomenon.

In Southeast Asia, the coalescence of high fossil fuel consumption, dense population, and agricultural intensification presents a potent recipe for atmospheric chemical loading. The island of Java, Indonesia, typifies this scenario. Despite its location in a humid equatorial belt, where rainfall is abundant and frequent [19], [20], recent evidence suggests that Java's wet deposition may be more chemically aggressive than previously acknowledged [21], [22]. Sulfate (SO_4^{2-}) and nitrate (NO_3^-), typically associated with industrial and vehicular emissions, have been found in concentrations rivaling those reported in industrial East Asia [23]. Moreover, ammonium (NH_4^+), a by-product of regional fertilizer uses and biomass burning, adds further complexity by modulating rainwater acidity through incomplete neutralization [24], [25]. This raises critical questions about the chemical composition of rainwater and the

ecological relevance of deposition fluxes under tropical climatic regimes.

Rainwater chemistry in tropical monsoonal settings defies simple hydrological logic. High rainfall volumes are often presumed to dilute pollutants effectively. In reality, the timing and intensity of precipitation relative to emission episodes create conditions where rainfall can act as a short-term amplifier of deposition rather than a neutralizer [26], [27]. For instance, post-dry-season rain events frequently scavenge concentrated aerosol layers, leading to episodic yet ecologically significant acid loads. In the absence of fine-resolution, event-based monitoring, such pulses remain undetected in conventional monthly or seasonal datasets. This data resolution gap limits the ability to capture threshold exceedances or to model the relationship between rainfall variability and ionic loading with sufficient spatial or temporal accuracy.

Despite the growing concern, rainwater monitoring efforts in Indonesia remain sparse and poorly integrated into environmental management frameworks [28]–[38]. Existing datasets are often temporally aggregated and spatially fragmented, precluding robust inference on ecological risk or emission linkages. Moreover, few investigations explicitly assess how the chemistry of rainwater interacts with monsoonal cycles or whether observed concentrations breach ecological risk thresholds. Without these critical perspectives, it becomes difficult to judge the environmental significance of deposition patterns or to formulate region-specific mitigation strategies.

This study addresses these deficiencies by analyzing a five-year (2019–2023), event-based dataset of rainwater chemistry collected from thirteen strategically distributed monitoring stations across Java Island, Indonesia. The objectives of this study are to: (1) characterize the spatial and seasonal variability of rainwater acidity and major ion concentrations; (2) evaluate the relationship between rainfall volume and ion concentrations using linear mixed-effects modeling; and (3) assess the frequency of ecological threshold exceedance related to acid deposition. Weekly observations of pH, SO_4^{2-} , NO_3^- , NH_4^+ , Cl^- , and rainfall volume were examined through spatial mapping, seasonal disaggregation, and hierarchical linear mixed-effects modeling to account for station-specific variability and temporal clustering. The analysis emphasizes the episodic nature of acid deposition in a tropical monsoonal regime, where pollutant build-up during dry spells is rapidly mobilized by early rainfall events. In addition to characterizing spatial and seasonal patterns, the study assesses the frequency of ecological threshold exceedance, providing quantitative insight into the environmental significance of deposition loads [39], [40]. By integrating high-resolution data with a

statistically rigorous framework, this research contributes a replicable methodology for atmospheric deposition assessment in data-limited tropical regions.

In doing so, the study not only advances empirical understanding of rainwater chemistry in tropical regions but also contributes methodologically by demonstrating the value of high-temporal-resolution sampling and hierarchical modeling in atmospheric deposition studies. By applying a mixed-effects modeling framework [41], [42], the analysis captures spatial heterogeneity and quantifies the influence of rainfall dynamics on pollutant concentrations, a dimension rarely explored in equatorial regions. The results directly challenge the prevailing notion that tropical rainfall inherently mitigates pollution and instead reveal a recurrent pattern of threshold exceedance linked to dry-season accumulation and monsoonal washout. These insights underscore the importance of incorporating wet deposition into national air quality standards and support the development of early warning and mitigation systems across Southeast Asia's rapidly urbanizing landscapes.

2. Methods

Study area and data collection. This study was conducted across Java Island, Indonesia, a region characterized by complex topography and a tropical monsoonal climate. The island, located between approximately 6°N to 9°S latitude and 105°E to 114°E longitude, experiences distinct wet and dry seasons influenced by the Asian-Australian monsoon system. Java's combination of coastal plains, mountainous interiors, and urbanized centres provides a diverse atmospheric environment for investigating wet deposition processes.

Rainwater samples and associated rainfall volume measurements were collected from thirteen monitoring stations strategically distributed across western, central, and eastern Java. The stations encompass various geographic and anthropogenic settings, including urban, suburban, and peri-urban locations. Rainwater was sampled using standard Wet Deposition or Wet & Dry Deposition methods, depending on the station instrumentation. All sites were equipped with Automatic Rain Water Samplers (ARWS) placed in open, unobstructed areas. A minimum of 200 mL of rainwater was required for complete ionic analysis. Samples were transferred to high-density polyethylene (HDPE) bottles and stored at 4°C prior to laboratory analysis. Ionic concentrations, including SO_4^{2-} , NO_3^- , NH_4^+ , and Cl^- , were analyzed using ion chromatography at the BMKG air quality laboratory. Detailed information on each station's geographic coordinates, land cover characteristics, and national land classification code (RBI) is summarized in Table 1..

Table 1. Monitoring station metadata including coordinates, land cover, and RBI land classification code

No	Station Name	Latitude	Longitude	RBI Code	Land Use / Land Cover (LULC)
1	Tangerang	-6.1	106.38	20093	Cropland – Irrigated (Paddy Field)
2	Tangerang Selatan	-6.26151	106.75084	2012	Urban and Built-up Land
3	Serang	-6.11185	106.11	20091	Rainfed Cropland
4	Kemayoran	-6.15559	106.84	2012	Urban and Built-up Land
5	Bandung	-6.88356	107.59733	2012	Urban and Built-up Land
6	Bogor	-6.5	106.75	20091	Rainfed Cropland
7	Cibeureum	-6.71074	106.95	20091	Rainfed Cropland
8	Semarang	-6.9847	110.3812	2012	Urban and Built-up Land
9	Tegal	-6.86817	109.12103	2012	Urban and Built-up Land
10	Cilacap	-7.7189	109.0149	2012	Urban and Built-up Land
11	Yogyakarta	-7.82	110.3	20091	Rainfed Cropland
12	Mlati	-7.731	110.354	20093	Cropland – Irrigated (Paddy Field)
13	Malang	-7.9008	112.5979	20093	Cropland – Irrigated (Paddy Field)
14	Juanda	-7.3846	112.7833	20121	Airports/Ports (Built-up)

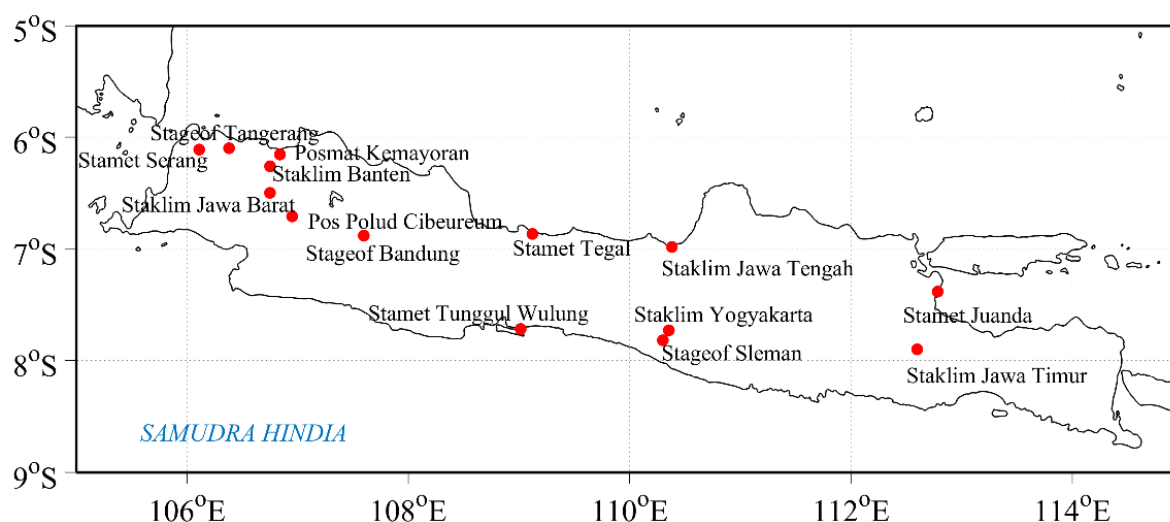


Figure 1. Location of the thirteen rainwater monitoring stations across Java Island, Indonesia. The sites include a mix of meteorological and climatological stations situated in urban, suburban, and peri-urban areas, spanning western to eastern parts of the island.

Weekly observations were recorded from January 2019 to December 2023, with chemical analyses conducted only during weeks when rainfall events occurred. Parameters measured included pH, electrical conductivity (represented as DH), and concentrations of major ions: calcium (Ca^{2+}), magnesium (Mg^{2+}), sodium (Na^+), potassium (K^+), ammonium (NH_4^+), chloride (Cl^-), sulphate (SO_4^{2-}), and nitrate (NO_3^-).

Due to the event-based nature of sampling, temporal gaps exist corresponding to weeks without precipitation. This dataset structure reflects the natural periodicity of rainfall in the monsoon-dominated tropics [19], [20] and provides a unique opportunity to investigate the short-term dynamics of wet deposition linked to individual rainfall events.

The geographical distribution of the monitoring stations is illustrated in Figure 1. The stations span the full longitudinal extent of Java Island, capturing coastal, inland, and highland environments. This spatial arrangement enables the assessment of wet deposition processes across diverse atmospheric and topographical conditions. Spatial patterns of median parameter concentrations were visualized using station-wise aggregation without interpolation, allowing direct comparison of deposition intensity across observed locations. The figure also highlights the proximity of several stations to major urban centres and industrial regions, offering further insights into potential anthropogenic influences on rainwater chemistry.

Data pre-processing and quality control. Prior to analysis, the dataset underwent a systematic pre-

processing workflow to ensure consistency and analytical validity. Given the event-based nature of the data, only weeks with recorded rainfall and corresponding chemical measurements were retained. Weeks with incomplete ion concentration data or missing rainfall volume values were excluded from the analysis to prevent bias in model estimations.

Outlier screening was performed to identify and remove physiochemically implausible values. Thresholds for acceptable ranges of each parameter were guided by established literature and region-specific climatological baselines [18], [26]. Any extreme values identified as likely due to instrumentation or recording errors were removed from the dataset to maintain integrity. Units of measurement were harmonized across all parameters, and ion concentrations were converted to milligrams per litre (mg/L) where necessary to ensure comparability.

In total, eleven physicochemical parameters were recorded from the rainwater samples, including pH, sulphate (SO_4^{2-}), nitrate (NO_3^-), chloride (Cl^-), ammonium (NH_4^+), calcium (Ca^{2+}), magnesium (Mg^{2+}), potassium (K^+), sodium (Na^+), electrical conductivity (EC), and cumulative rainfall (CH). For the purpose of core spatial and statistical analysis, six parameters—pH, SO_4^{2-} , NO_3^- , Cl^- , NH_4^+ , and CH—were selected. These were prioritized based on their relevance to acid deposition processes, distinct source signatures, and consistent spatial patterns across the monitoring network. The remaining parameters were retained for secondary analysis and validation purposes, although not highlighted in the main results.

To facilitate interstation comparisons and preserve the temporal resolution of weekly observations, all data were standardized to a common weekly time base. No interpolation was performed for missing rainfall events, preserving the integrity of the event-driven dataset. Spatial summaries and seasonal statistics were derived from concurrent observations across stations at each time step. An example of the cleaned and structured data is presented in Figure 2, showing weekly rainfall volume and sulphate concentration from the Tangerang station. The episodic nature of precipitation in the study region is clearly visible, as are short-term fluctuations in ion concentrations, supporting the decision to analyze deposition chemistry as a dynamic, non-continuous process.

Statistical and modelling approach. The analytical framework of this study aimed to characterize the spatiotemporal variability of rainwater chemistry and evaluate its relationship with rainfall volume under monsoonal influences. Descriptive statistical analyses were conducted to summarize central tendency, dispersion, and seasonal variation in ionic concentrations and rainfall across the 13 stations. Boxplots and time series visualizations were generated to illustrate interstation differences and highlight seasonal trends.

Associations between rainfall volume and ion concentrations were explored using bivariate correlation analysis. Depending on the distributional properties of the variables, both Pearson and Spearman correlation coefficients were applied, following best practices in hydrometeorological statistics [42]. These analyses provided an initial understanding of linear and monotonic relationships between precipitation intensity and chemical loads.

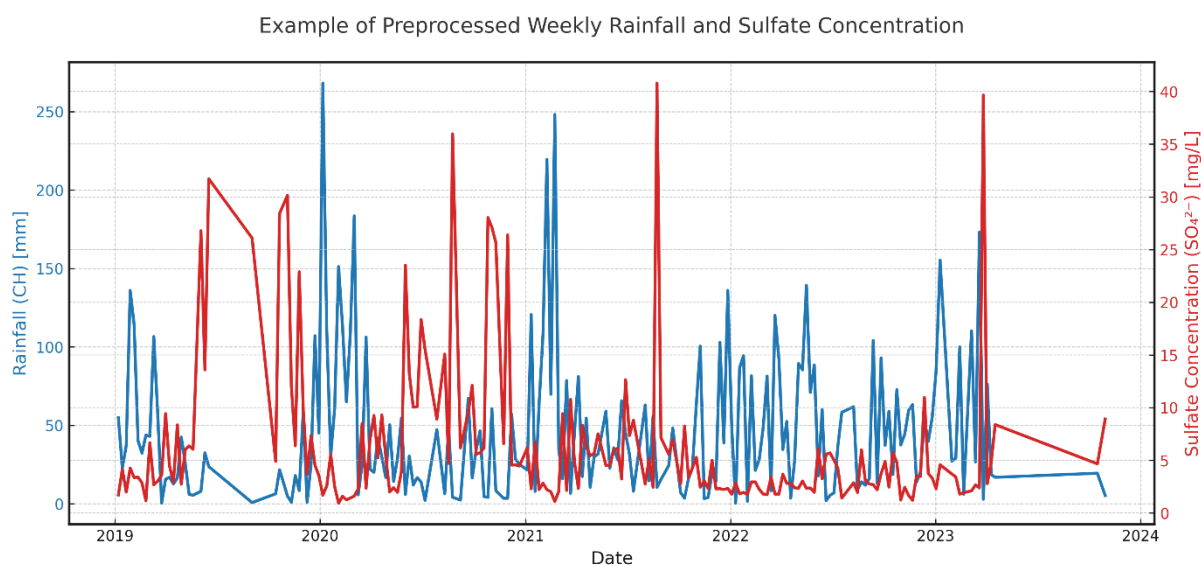


Figure 2. Time series of pre-processed weekly rainfall volume (CH) and sulphate concentration (SO_4^{2-}) from Tangerang station. The data illustrate event-based sampling, where observations are recorded only during rainfall weeks. Variability in ion concentration reflects both atmospheric inputs and dilution effects.

To quantify the influence of rainfall volume on ion concentrations while addressing the hierarchical structure of the dataset (i.e., repeated weekly observations within the same station), we employed linear mixed-effects (LME) models for each key rainwater parameter (pH, SO_4^{2-} , NO_3^- , NH_4^+ , Cl^-). The LME framework was chosen due to its ability to partition variance between fixed effects (rainfall volume, CH) and random effects (station-specific variability), thus capturing both population-level and location-specific relationships. This model structure is appropriate for unbalanced, nested, or longitudinal data and follows the formulation in Pinheiro and Bates[41].

$$Y_{ij} = \beta_0 + \beta_1 \cdot CH_{ij} + b_{0j} + \varepsilon_{ij} \quad (1)$$

Y_{ij} is the ion concentration at time i in station j , CH_{ij} is the rainfall volume, β_0 and β_1 are fixed-effect intercept and slope, b_{0j} is the random intercept for station j , and ε_{ij} is the residual error.

This formulation accounts for intra-station correlation and heterogeneity, enabling more robust estimation of rainfall effects across spatially diverse environments. Model performance was evaluated using significance levels (t-tests for fixed effects), estimated variance components, and model fit statistics. Although generalized additive models (GAMs) were initially considered, LME models offered better interpretability and comparable predictive power, justifying their selection.

Although generalized additive models (GAMs) were initially tested to evaluate potential nonlinear relationships between rainfall and ionic parameters, they were not retained in the final analysis due to comparable performance with LME models and less interpretability. The LME framework was therefore preferred for its balance of explanatory power and analytical clarity.

Seasonal stratification was conducted by categorizing weeks into four meteorological seasons: DJF (Dec–Jan–Feb), MAM (Mar–Apr–May), JJA (Jun–Jul–Aug), and SON (Sep–Oct–Nov). This enabled comparative analysis of rainwater chemistry under distinct climatic regimes[19]. Threshold values for risk assessment, such as $\text{pH} < 5.6$, $\text{SO}_4^{2-} > 5 \text{ mg/L}$, and $\text{NO}_3^- > 2 \text{ mg/L}$, were selected based on environmental standards and prior studies on acid deposition impacts [18], [39], [40].

3. Result

Descriptive analysis. Rainwater chemistry in the study region was examined using six key parameters: pH, sulphate (SO_4^{2-}), nitrate (NO_3^-), ammonium (NH_4^+), chloride (Cl^-), and cumulative rainfall (CH). These variables represent a spectrum of atmospheric processes, from acidifying components (SO_4^{2-} , NO_3^-) and neutralizing agents (NH_4^+) to halide influence (Cl^-) and precipitation dynamics (CH). pH serves as

a net indicator of ionic balance, modulated by both anthropogenic and natural emissions.

Inter-station variability in these parameters is visualized in Figure 3, which presents the boxplots of weekly measurements across 13 monitoring stations. To enhance interpretability, the stations on each plot were ordered based on their ascending median values, allowing for a direct visual comparison of central tendency and dispersion across sites. This approach helps prioritize stations with the highest and lowest chemical loads in each parameter and reinforces spatial contrasts in rainwater composition.

pH values varied widely among stations, with observed medians ranging approximately from 4.7 to 6.8. Stations classified as urban or peri-urban, such as Kemayoran, Bandung, and Juanda, consistently recorded lower pH values, often dipping below 5.6, an established threshold for acid rain episodes[18]. In contrast, higher median pH levels were observed at stations like Cibereum, Cilacap, and Mlati, which are situated in agricultural or mixed-use areas. This contrast suggests the presence of alkaline buffering agents, possibly from local dust or ammonia emissions. These spatial patterns align with the land use categorization presented in Table 1, and indicate that differences in site-level land cover significantly influence rainwater acidity.

Among the ionic constituents, SO_4^{2-} and NO_3^- were dominant anions, with maximum weekly concentrations exceeding 6 mg/L at some urban sites. These values are notably higher than background levels typically reported in low-impact areas, where sulfate and nitrate concentrations generally remain below 2–3 mg/L and 1–2 mg/L, respectively [18], [44]. The elevated concentrations observed in urban stations reinforce the role of fossil fuel combustion, vehicular emissions, and industrial activities as major contributors to acidifying wet deposition in the study region. Stations located in densely populated and industrialized corridors, particularly Kemayoran (Jakarta) and Bandung, exhibited pronounced upper quartiles and frequent extreme values. These patterns point to contributions from fossil fuel combustion, vehicular emissions, and other anthropogenic sources, as widely documented in previous regional studies [43], [44].

NH_4^+ concentrations showed notable variability, with elevated medians at Mlati and Karanganyar, likely influenced by agricultural activities such as urea-based fertilizer volatilization, and at Tangerang, where urban emissions including waste decomposition and traffic-related sources may contribute to ammonium loading.

Chloride (Cl^-) displayed mixed spatial signatures. While high concentrations were anticipated in coastal sites like Tegal, Cilacap, and Surabaya, several inland stations also registered moderate levels, potentially linked to biomass burning or industrial emissions.

This dual-origin signature reflects the complex interaction of marine and land-based aerosol sources.

Cumulative rainfall (CH) showed wide distribution across stations, from weekly medians below 40 mm in northern lowland areas to above 100 mm in orographic and southern coastal regions. This variation is indicative of topographical influences and spatial gradients in monsoonal precipitation intensity.

Collectively, Figure 3 highlights both the magnitude and variability of wet deposition parameters across Java. Skewed distributions and the presence of outliers at several stations point to episodic atmospheric events or localised emission spikes. Importantly, the boxplots emphasize that central tendency measures (e.g., median) may obscure short-term but environmentally significant extremes,

particularly in stations subject to complex emission regimes. These findings underscore the need for spatially-explicit analysis, which is pursued further in the following section through mapped representations of median values.

To provide numerical context beyond the boxplot visualization, Table 2 presents the mean (ave), minimum, and maximum values of pH, major ions, and rainfall volume at each station. These summary statistics complement Figure 3 by quantifying the spatial heterogeneity described above, and are particularly useful for identifying extreme values and station-level contrasts not easily inferred from median-based graphics alone.

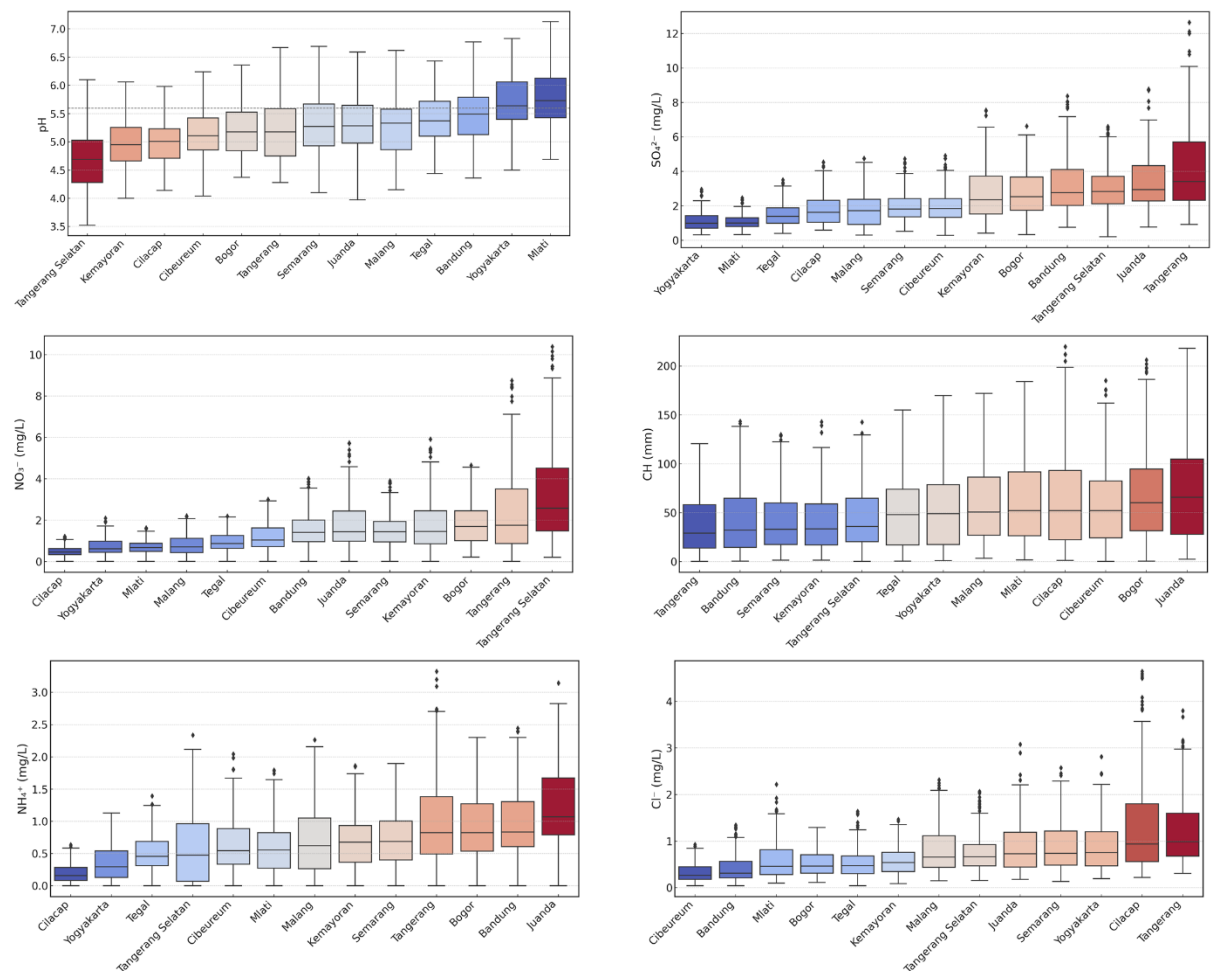


Figure 3. Boxplots of weekly rainwater parameters across thirteen monitoring stations in Java Island, Indonesia, arranged in a 3×2 layout for improved readability. Parameters include rainwater pH, sulfate (SO₄²⁻), nitrate (NO₃⁻), ammonium (NH₄⁺), chloride (Cl⁻), and cumulative rainfall (CH). Stations are ordered by ascending median value for each parameter, and color gradients from blue to red reflect the increasing median. Outliers are hidden for visual clarity..

Table 2. Descriptive statistics (mean, minimum, and maximum) for pH, sulfate (SO₄²⁻), nitrate (NO₃⁻), ammonium (NH₄⁺), chloride (Cl⁻), and cumulative rainfall (CH) at 13 monitoring stations across Java Island (2019–2023). Values are calculated from weekly event-based observations.

Station	PH			SO ₄ ²⁻ (mg/L)			NO ₃ ⁻ (mg/L)			NH ₄ ⁺ (mg/L)			Cl ⁻ (mg/L)			Rainfall (mm)		
	ave	min	max	ave	min	max	ave	min	max	ave	min	max	ave	min	max	ave	min	max
Tangerang	5.2	4.3	6.7	6.4	0.9	40.8	4.4	0	36.2	1.4	0	7.2	2	0.3	22.3	45.9	0.4	268.1
Tangerang Selatan	4.7	3.5	6.4	3.3	0.2	16.3	4	0.2	29.3	0.7	0	3.8	1.2	0.2	19.3	57.4	0.2	277.8
Kemayoran	5	4	6.3	3.4	0.4	16.6	2.3	0	14.9	0.9	0	10.1	0.9	0.1	6.8	59.4	1.6	410.2
Bandung	5.5	4.4	7.2	4.3	0.8	45.7	2.4	0	43.7	1.1	0	5.1	1	0	22.2	50	0.5	214.9
Bogor	5.2	4.4	6.9	3	0.3	20.9	2.2	0.2	26.9	1	0	5.6	0.6	0.1	4.5	79.5	0.5	358.9
Cibeureum	5.2	4	6.4	2.8	0.3	38.7	1.9	0	33.1	0.9	0	8	0.6	0	11.9	71.1	0.4	269.9
Semarang	5.4	3.7	7.3	2.7	0.5	37.9	1.9	0	9.5	0.8	0	2.7	1.3	0.1	13.1	51.1	1.4	358.6
Tegal	5.4	4.4	6.4	1.8	0.4	15.9	1.3	0	18.3	0.6	0	3.3	0.9	0	18.4	59.6	0.6	294.8
Cilacap	5	4.1	6.6	2	0.6	19	0.7	0	7.3	0.3	0	2.2	2.6	0.2	61.5	77.8	1.2	465.7
Yogyakarta	5.7	3.9	7.5	1.5	0.3	15.2	1.2	0	32.1	0.5	0	4.5	2	0.2	40.3	57.7	1	242
Mlati	5.8	4.7	7.2	1.3	0.3	9.7	1	0	14.7	0.7	0	4.5	1.1	0.1	16.6	65.7	1.7	227
Malang	5.3	4.2	6.8	1.9	0.3	6.4	0.9	0	3.8	0.8	0	4.8	1.7	0.2	108.9	62.1	3.5	239.1
Juanda	5.3	3.7	6.6	6.4	0.8	92	2.5	0	32.6	1.4	0	5.6	2.1	0.2	23.7	79.4	2.5	308

Spatial patterns of ion concentrations and rainfall.

The spatial distributions of median concentrations for key rainwater parameters across Java, as illustrated in Figure 4, reveal distinct geographic patterns that reflect a combination of meteorological influences and localized anthropogenic sources. These patterns are particularly informative for understanding the atmospheric processes shaping wet deposition chemistry in a tropical monsoonal setting.

Sulphate (SO₄²⁻) and nitrate (NO₃⁻) concentrations were consistently higher in western urban-industrial corridors, particularly around Tangerang (B), Bandung (G), and Kemayoran (C). These areas are heavily trafficked, densely populated, and host significant industrial activities. SO₄²⁻ is commonly associated with secondary aerosol formation from sulfur dioxide (SO₂), largely emitted by fossil fuel combustion in power plants and industrial boilers. Likewise, NO₃⁻ originates predominantly from the oxidation of nitrogen oxides (NO_x), a by-product of vehicular emissions and combustion processes. Such source pathways have been well-documented in tropical and subtropical Asia [18], [45], with studies in urban Indonesia also attributing high sulfate burdens to coal-dominated power generation [23].

In contrast, elevated ammonium (NH₄⁺) levels were observed inland, particularly in agricultural zones such as Cibeureum (F), Karanganyar (J), and Yogyakarta (K–L). These concentrations are indicative of intensive fertilizer use, which contributes ammonia (NH₃) through volatilization, especially from urea-based inputs and animal waste [24], [46]. Once emitted, NH₃ reacts with acidic species to form particulate NH₄⁺, which is readily scavenged by rain. The spatial overlap of NH₄⁺ with rural-agrarian settings in this study suggests a distinct nitrogen deposition pathway that is less prominent in urban stations.

Chloride (Cl⁻) displayed a relatively dispersed pattern, with moderate levels both in northern coastal areas (Serang – A; Tegal – H) and southern coasts (Cilacap – I). These concentrations may arise from a mixture of marine aerosol intrusion and re-suspension of de-icing salts or dust from road surfaces in densely traveled regions [47]. The inland presence of Cl⁻ away from direct marine influence implies additional anthropogenic contributions, possibly linked to combustion or waste-related sources.

The spatial distribution of rainwater acidity (as inferred from pH) further highlights the cumulative effect of acid-forming species. Stations with elevated SO₄²⁻ and NO₃⁻ concentrations tended to exhibit lower pH values, particularly in Jakarta (C) and Banten (D). While both are situated in the western urban corridor of Java, their local settings differ: Kemayoran in Jakarta is characterized by dense high-rise development and coastal influence, which may promote vertical air mixing and marine aerosol buffering. In contrast, Staklim Banten is located in a semi-residential inland area where emissions from household combustion and limited atmospheric dispersion may lead to higher accumulation of acid precursors. This spatial coupling aligns with acid rain formation mechanisms, where strong inorganic acids dominate the neutralization balance due to insufficient alkaline buffering from base cations like Ca²⁺ or Mg²⁺ [43]. In contrast, stations in central Java showed higher pH values, possibly due to increased dust or biogenic alkalinity.

Cumulative rainfall (CH) showed considerable variation across the island, with the highest median values observed in orographically influenced regions such as Cilacap (I), Yogyakarta (K), and Sleman (L). These patterns are consistent with the spatial signature of Java's monsoonal rainfall, where convective uplift and windward slopes enhance

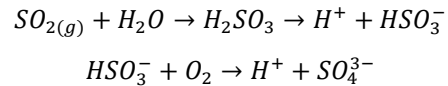
precipitation [19], [20]. Interestingly, some of these high-rainfall areas also showed elevated ion concentrations, suggesting that wet scavenging did not necessarily dilute ionic loads but rather captured episodic pollution events—likely from biomass burning or traffic surges during dry-to-wet season transitions.

The coexistence of diverse chemical zones—urban-industrial, agricultural, and coastal—underscores the heterogeneous nature of atmospheric deposition across Java. The clear spatial compartmentalization of SO_4^{2-} , NO_3^- , and NH_4^+ in particular suggests the feasibility of using deposition chemistry as an environmental diagnostic tool to monitor emission sources and inform local mitigation strategies. Targeted reduction of SO_2 and NO_x through clean energy transitions in urban corridors, coupled with sustainable nitrogen management in farming regions, could significantly alter the chemical burden of wet deposition in the region.

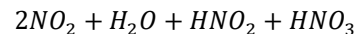
Atmospheric mechanisms and ionic interactions.

The chemical composition of rainwater is shaped by complex atmospheric processes involving gas-to-particle conversion, cloud chemistry, and in-cloud or below-cloud scavenging. An important aspect of interpreting wet deposition data lies in understanding how ionic species interact with one another and with rainfall dynamics.

The observed acidity of rainwater, as indicated by pH values frequently below 5.6, suggests strong influence from inorganic acid precursors—primarily sulfur dioxide (SO_2) and nitrogen oxides (NO_x). These gases undergo atmospheric oxidation through both gas-phase and aqueous-phase pathways. For instance, SO_2 can be oxidized in cloud water via:



Similarly, nitrogen oxides (mainly SO_2) form nitric acid through:



These acids dissociate in rainwater, increasing the H^+ ion concentration and thus lowering the pH. The resulting sulfate SO_4^{2-} and nitrate NO_3^- ions readily dissolve into cloud droplets or are scavenged by falling raindrops, contributing to acid deposition.

The extent of acidification is modulated by the presence of neutralizing agents, particularly ammonium (NH_4^+), which originates from ammonia (NH_3) emitted by agricultural activities. This NH_3 can neutralize acidic species via reactions such as:

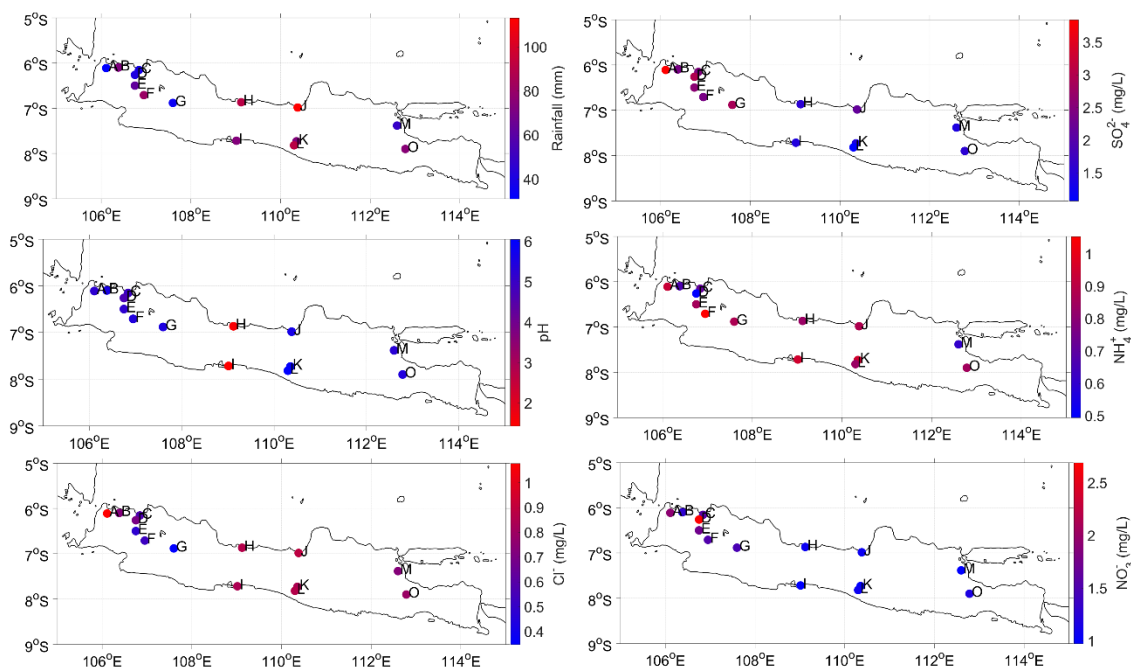
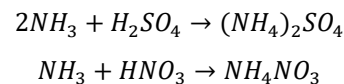


Figure 4. Median spatial distribution of six rainwater parameters (pH, SO_4^{2-} , NO_3^- , NH_4^+ , Cl^- , CH) across Java. Color gradients indicate relative concentrations or volume, with each station labeled A–O for clarity. Station codes: A. Stamet Serang, B. Stageof Tangerang, C. Posmet Kemayoran, D. Staklim Banten, E. Staklim Jawa Barat, F. Pos Polud Cibureum, G. Stageof Bandung, H. Stamet Tegal, I. Stamet Tunggul Wulung, J. Staklim Jawa Tengah, K. Staklim Yogyakarta, L. Stageof Sleman, M. Stamet Juanda, O. Staklim Jawa Timur.

These reactions form stable salts, which reduce rainwater acidity. However, the buffering effect is spatially variable and often insufficient in heavily urbanized environments, where the spatial co-occurrence of low pH values and elevated SO_4^{2-} and NO_3^- concentrations (see Figure 4) reflects the dominance of combustion-related emissions in these regions [18], [43].

However, the extent of acidification is modulated by the presence of neutralizing agents, particularly ammonium (NH_4^+). Formed via atmospheric uptake of ammonia (NH_3)—itself largely sourced from fertilizers and livestock— NH_4^+ can react with acidic species to form ammonium sulfate or ammonium nitrate, thereby buffering rainwater acidity. This buffering is evident in several agricultural stations where high NH_4^+ levels appear to coincide with relatively moderate pH, despite measurable sulfate and nitrate concentrations. This interaction supports findings from previous work in tropical monsoon regions, where NH_4^+ is often the dominant cation contributing to neutralization capacity [24], [26].

Nevertheless, this buffering is not always sufficient. In some stations, such as Kemayoran or Bandung, acidity remains high even in the presence of NH_4^+ . This could be attributed to an imbalance between acid loading and base availability, or to the predominance of stronger acids over NH_4^+ buffering capacity. Additionally, studies have shown that NH_4^+ neutralization is more effective when coupled with basic crustal cations like Ca^{2+} or Mg^{2+} [25], which may be limited in urban air masses.

Rainfall volume (CH) further complicates these interactions. Theoretically, greater precipitation should dilute ionic concentrations via washout (below-cloud scavenging) and rainout (in-cloud scavenging). However, our data show that regions with higher rainfall—such as Cilacap, Yogyakarta, and Sleman—do not necessarily exhibit lower ionic concentrations. This suggests that heavy precipitation may in fact coincide with episodic pollution events, or that it efficiently scavenges a large atmospheric burden, especially during the onset of monsoon transition phases. This is consistent with observations in Southeast Asian urban zones, where rain events often coincide with high PM levels following dry spells [26].

Collectively, these findings highlight the dual role of rainfall: both as a cleansing mechanism and as an effective transporter of accumulated atmospheric pollutants. Moreover, they emphasize the nonlinear

relationship between deposition chemistry and meteorological variables in monsoon-influenced tropical climates. This complexity reinforces the importance of evaluating multiple chemical species jointly, rather than in isolation, to understand the atmospheric drivers of rainwater chemistry.

To further elucidate these chemical interactions, Figure 5 presents scatterplots of selected bivariate relationships among pH, ionic species, and rainfall volume. The insights derived from bivariate interactions among rainwater parameters reinforce the interpretations of underlying atmospheric mechanisms. Figure 5 presents scatterplots illustrating three key relationships: pH vs SO_4^{2-} , pH vs NH_4^+ , and rainfall volume (CH) vs total ionic concentration.

Panel (a) of Figure 5 reveals an expected inverse relationship between sulphate and pH, where increasing SO_4^{2-} is typically associated with decreasing rainwater pH. This aligns with established understanding of sulphuric acid as a principal contributor to acid precipitation, particularly in environments affected by fossil fuel combustion and industrial emissions [18], [43]. The wide range of SO_4^{2-} concentrations, spanning nearly two orders of magnitude, underscores spatial heterogeneity in acid precursor inputs.

Panel (b) explores the interaction between ammonium and pH. While a clear linear trend is absent, clusters of data points suggest that moderately elevated NH_4^+ levels can correspond with less acidic conditions, consistent with the role of NH_4^+ as a neutralizing agent. However, the buffering capacity appears uneven, reinforcing the notion that NH_4^+ alone is insufficient to counterbalance high acid loading without the presence of additional base cations such as Ca^{2+} or Mg^{2+} [24], [25].

Panel (c) examines the relationship between rainfall volume and total ion concentrations. The expected dilution effect of higher precipitation is not clearly observed; instead, the relationship appears weak or even mildly positive. This may reflect the dual role of rainfall in both scavenging atmospheric aerosols and transporting freshly emitted pollutants. In tropical regions with intense convective events, heavy rainfall may coincide with large-scale uplift and washout of accumulated pollutants, rather than simply diluting existing concentrations [26]. Thus, total ion loading in rainwater does not always decrease with greater rainfall, a finding consistent with previous studies in monsoon-influenced environments.

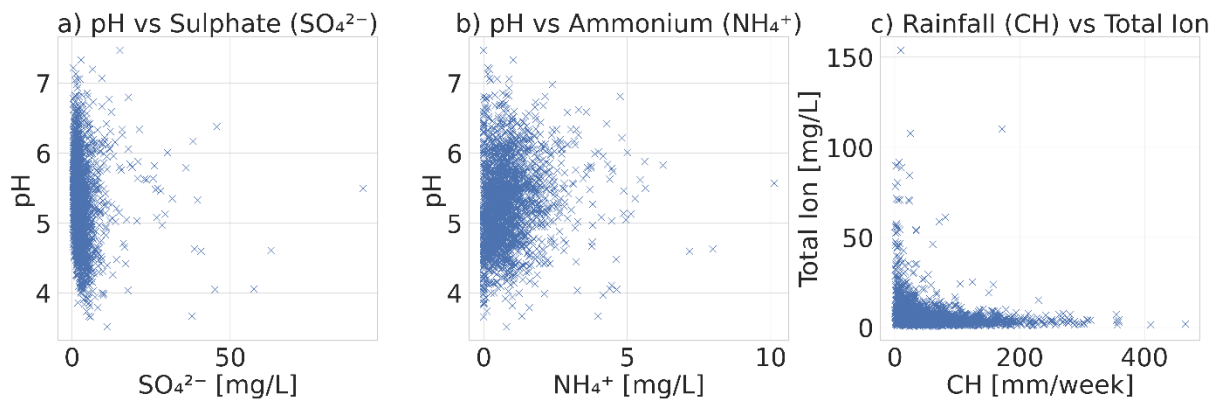


Figure 5. Scatterplots illustrating key interactions in rainwater chemistry: a) pH vs Sulphate (SO_4^{2-}), b) pH vs Ammonium (NH_4^+), and, c) Rainfall volume (CH) vs Total ion concentration ($\text{SO}_4^{2-} + \text{NO}_3^- + \text{NH}_4^+ + \text{Cl}^-$).

Modeling spatial variability: Linear Mixed Effects. To quantify the influence of rainfall on rainwater chemistry while accounting for site-specific heterogeneity, linear mixed effects (LME) models were fitted for each major parameter using weekly rainfall (CH) as a fixed effect and station identity as a random intercept. The results, summarized in Table 1, indicate that CH significantly predicts the variability in all five parameters analyzed, pH, SO_4^{2-} , NO_3^- , NH_4^+ , and Cl^- , with negative coefficients across the board.

The inverse relationship between CH and ionic concentrations aligns with established washout theory, wherein increased precipitation dilutes atmospheric ionic loads through scavenging mechanisms [43]. Specifically, SO_4^{2-} and NO_3^- exhibited the strongest responses to rainfall variation, with highly significant coefficients ($p < 0.001$), suggesting that acidic species are particularly sensitive to episodic precipitation. This reflects the dominance of wet deposition in modulating acidic inputs in tropical monsoonal settings, where rainfall variability governs the rate and extent of atmospheric cleansing [18].

The model also revealed that ammonium (NH_4^+) and chloride (Cl^-) concentrations decreased with increasing CH, reinforcing the hypothesis that these ions, commonly associated with agricultural emissions and marine or urban sources, respectively,

are susceptible to rain-mediated removal [48]. While the estimated effect of CH on pH was relatively weaker ($p = 0.048$), it remained statistically significant, suggesting that rainfall also modulates overall acidity, albeit with more complex buffering interactions.

Importantly, the random effect variances underscore the substantial interstation variability, validating the use of LME as opposed to fixed-effect models. This station-specific heterogeneity likely reflects localized emission profiles, meteorological microenvironments, and surface characteristics—factors that simple regression models cannot capture adequately [47]. The mixed model framework thus provides a robust analytical lens to reconcile the competing influences of large-scale precipitation events and local context.

Collectively, the modeling results affirm the hypothesis that rainfall plays a pivotal role in shaping the spatial and temporal dynamics of rainwater chemistry across Java. Beyond supporting the patterns visualized in Figures 3–5, these findings lend statistical rigor to the interpretation of depositional processes and offer a quantitative basis for spatial risk assessment.

Table 1. Summary of LME models for rainfall effects on rainwater chemistry parameters.

Parameter	Estimate (CH)	Std Error	t-value	p-value	Random Effect Var
pH	-0.0004	0.0002	-1.98	0.048	0.0785
SO4	-0.0167	0.0016	-10.66	0.0	2.6067
NO3	-0.0128	0.0011	-11.22	0.0	1.1091
NH4	-0.0041	0.0003	-14.66	0.0	0.1295
CL	-0.0077	0.0013	-5.84	0.0	0.3364

Seasonal differences in rainwater chemistry.

Beyond spatial heterogeneity, the chemical composition of rainwater in Java is also subject to temporal modulation driven by seasonal atmospheric dynamics. The previous sections have elucidated site-specific contrasts shaped by urbanization, topography, and emission profiles. However, the monsoonal climate of Indonesia imposes a recurrent rhythm of wet and dry periods that alters emission fluxes, convective activity, and pollutant transport. Investigating how rainwater chemistry varies across seasons is thus essential to understand the interplay between meteorological regimes and atmospheric deposition. This section presents a temporal disaggregation of ionic concentrations and acidity, highlighting seasonal signatures that are often masked in aggregated spatial analyses.

Rainwater chemistry in Java exhibits clear seasonal modulation, shaped by the monsoonal cycle and associated atmospheric processes. Figure 6 synthesizes weekly observations from 2019 to 2023 into seasonal boxplots, revealing distinct differences in ionic concentrations and pH across DJF (Dec–Jan–Feb), MAM (Mar–Apr–May), JJA (Jun–Jul–Aug), and SON (Sep–Oct–Nov). The patterns suggest that rainfall seasonality, through both meteorological dynamics and emission timing, plays a pivotal role in governing the chemical burden of wet deposition.

Acidifying species such as sulfate (SO_4^{2-}) and nitrate (NO_3^-) were consistently elevated during the dry season (JJA) and early wet transition (SON), with median concentrations declining during DJF. This trend points toward two interrelated drivers. First, reduced precipitation frequency during JJA limits atmospheric cleansing, allowing pollutants from vehicular exhaust, industrial processes, and biomass burning to accumulate in the boundary layer [49], [50]. Second, dry-season emissions are often intensified by increased combustion activity, particularly in peri-urban and rural zones, contributing to elevated concentrations of acid precursors. During SON, the onset of convective rainfall mobilizes accumulated aerosols, leading to high episodic deposition. These findings align with chemical transport modeling studies that emphasize monsoon onset as a critical phase for aerosol washout and chemical transitions [27].

Ammonium (NH_4^+) exhibits a more complex seasonal signature. While its levels are also elevated in JJA and SON, the pattern is likely influenced by seasonal fertilizer application, livestock waste volatilization, and reduced rainfall dilution. NH_4^+ originates primarily from ammonia (NH_3), which is volatilized more rapidly in warm and dry conditions, especially in intensively cultivated landscapes [24], [46]. This atmospheric NH_3 readily reacts with acidic species to form particulate NH_4^+ , which is then removed via wet scavenging. The observed seasonal clustering

suggests that agricultural NH_3 emissions interact synergistically with acid loading, particularly during transition months.

Chloride (Cl^-) concentrations peak in JJA and SON, consistent with the behavior of sea salt aerosols transported inland during the dry season. However, given the inland elevation of several stations, this trend likely reflects anthropogenic contributions such as biomass combustion and solid waste incineration. Prior investigations in Southeast Asia have identified Cl^- as a marker of mixed marine and terrestrial sources, including open burning and industrial emissions [47], [51]. Its persistence across seasons indicates a stable input from regional sources, with heightened deposition during periods of lower rainfall frequency.

The pH of rainwater shows its lowest median values during JJA and SON, mirroring the seasonal peaks of sulfate and nitrate. This inverse relationship reflects the acidifying dominance of strong inorganic acids over neutralizing agents during the dry and transitional months. The absence of sufficient rainfall to remove accumulated pollutants during JJA exacerbates acid loading. Additionally, DJF, a period characterized by high rainfall volume and sustained convective activity, corresponds to relatively higher pH values, likely due to both dilution and enhanced buffering by crustal ions or NH_4^+ . The atmospheric transport of mineral dust and bioaerosols during wet seasons contributes further to alkalinity [25], [26].

Interestingly, cumulative rainfall (CH) itself follows the expected monsoonal rhythm, peaking sharply during DJF and tapering off through MAM and JJA. Yet, the dilution effect of rainfall on ion concentrations is not strictly proportional. Several parameters retain elevated concentrations even in the presence of substantial rainfall during SON, indicating that rain events may not dilute the atmosphere uniformly but instead mobilize concentrated plumes of pollutants accumulated during dry spells. This highlights the dual role of rainfall, as both a cleansing agent and a vehicle for pollution transfer, depending on its timing relative to emission buildup.

Taken together, the seasonal boxplots reveal the complexity of chemical–meteorological interactions in a tropical monsoonal regime. The nonlinearity between rainfall volume and ionic concentrations underscores the need to consider emission timing, atmospheric retention, and precipitation intensity jointly. These insights build upon foundational work on aerosol–rainfall interactions in Asia [18], [45], and provide empirical evidence that seasonal dynamics should be central to any modeling or mitigation strategy targeting acid deposition in Southeast Asian megaregions.

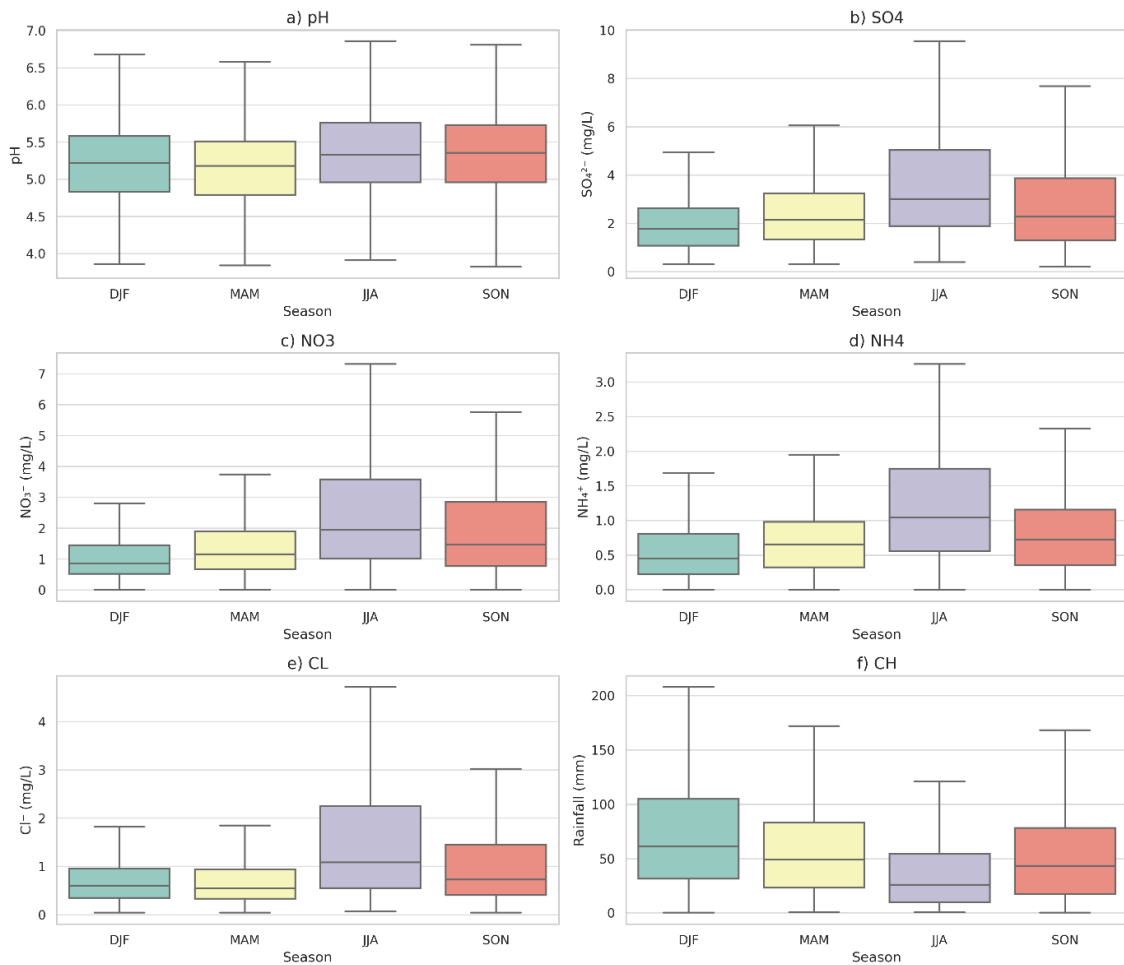


Figure 6. Seasonal distribution of rainwater chemistry parameters across Java Island, Indonesia, based on weekly measurements during 2019–2023. Each boxplot shows the interquartile range and median value of six parameters, pH, SO_4^{2-} (sulfate), NO_3^- (nitrate), NH_4^+ (ammonium), Cl^- (chloride), and CH (cumulative rainfall), classified into four meteorological seasons: DJF, MAM, JJA, and SON. Outliers are excluded to enhance visualization of central tendencies and dispersion.

Environmental significance based on threshold comparisons. While previous sections have detailed the spatial and seasonal variability of rainwater chemistry, they do not directly address the ecological significance of the observed concentrations. Understanding whether the measured ionic loads pose actual environmental risks requires comparison against scientifically recognized thresholds. Such comparisons provide essential context, translating concentrations from descriptive values into environmental meaning, and allow this study to speak not only to variability but also to impact.

To this end, three parameters were selected for threshold-based analysis: pH, sulfate (SO_4^{2-}), and nitrate (NO_3^-). These variables were chosen based on two criteria: (1) the existence of internationally recognized or ecologically validated benchmarks, and (2) their central role in acid rain formation and nitrogen-driven ecosystem stress. Other ions, such as ammonium (NH_4^+) and chloride (Cl^-), while abundant, lack universal environmental thresholds for

wet deposition and thus were excluded from this comparative risk framework.

Figure 7 presents the proportion of weekly rain events between 2019 and 2023 that exceeded critical environmental thresholds: $\text{pH} < 5.6$, $\text{SO}_4^{2-} > 5 \text{ mg/L}$, and $\text{NO}_3^- > 2 \text{ mg/L}$. The first threshold, $\text{pH} < 5.6$, is widely accepted as the baseline for acid precipitation, representing the point below which rain is no longer considered neutralized by atmospheric CO_2 alone [18]. Across Java, nearly half of all events ($\approx 47\%$) fell below this pH threshold, indicating frequent acid rain conditions even in a tropical environment where buffering is often presumed. This high frequency challenges assumptions that equatorial rainfall is consistently alkaline, and signals the presence of strong acidifying agents from anthropogenic combustion sources.

Sulfate, as the dominant acidifying anion derived from sulfur dioxide oxidation, showed concentrations above 5 mg/L in approximately 29% of samples. This level is considered ecologically hazardous, particularly for soils with low buffering capacity and

for foliar surfaces of crops and natural vegetation [39]. The fact that nearly one-third of events reach this level of sulfate loading suggests episodic but potent inputs from fossil fuel combustion, likely intensified during dry-season accumulation and monsoon onset washout, as previously discussed.

Nitrate concentrations exceeded the 2 mg/L threshold in about 34% of samples, raising concern over reactive nitrogen deposition. While nitrate is a nutrient, its atmospheric deposition in excess is linked to eutrophication, soil acidification, and groundwater contamination [40]. The prevalence of elevated NO_3^- levels in this study aligns with patterns of high vehicular density and fertilizer use, especially in peri-urban agricultural zones, indicating that nitrogen pollution in Java is not confined to terrestrial runoff but is actively transported and deposited via rain.

Together, these exceedance rates point to a nontrivial environmental burden. The convergence of high-frequency acid rain episodes and elevated deposition of sulfate and nitrate suggests that Java is experiencing atmospheric deposition loads that are environmentally consequential, not just statistically variable. Importantly, these findings demonstrate that rainwater chemistry in the region is not only modulated by meteorological patterns but also saturated with pollution to levels that cross ecological thresholds. This adds a new dimension to the narrative of Southeast Asian air pollution, one that implicates not only visibility and PM exposure, but also chronic, ecosystem-level acidification risks via precipitation.

The implications extend to agriculture, forestry, and freshwater systems, particularly in areas with inherently low buffering soils or intensive cropping systems. Further integration with soil pH data and crop response studies would be valuable in assessing the cumulative ecological risk posed by atmospheric deposition. In the absence of regulatory standards for wet deposition in Indonesia, these results also underscore the need to establish monitoring frameworks aligned with ASEAN or global acid deposition conventions.

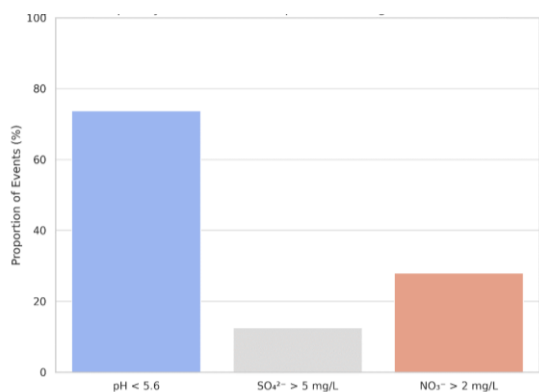


Figure 7. Frequency of Rainwater Samples Exceeding Environmental Thresholds [18], [39-40].

Interannual trends in rainwater chemistry (2019–2023). While the previous sections have focused on spatial patterns, seasonal differences, and threshold exceedances, understanding interannual variability is equally vital to assess long-term deposition dynamics and to inform sustainable environmental policies. To this end, we examined year-to-year trends across all monitoring stations for key rainwater parameters over the five-year observation period.

Figure 8 presents annual boxplots (2019–2023) for pH, sulfate (SO_4^{2-}), nitrate (NO_3^-), ammonium (NH_4^+), chloride (Cl^-), and cumulative rainfall (CH). These distributions reflect the central tendency, variability, and outliers of each parameter based on weekly observations pooled from all 13 monitoring stations.

Sulfate and nitrate, the two dominant acidifying anions, displayed clear peaks in 2020 and 2022, suggesting intensified acid deposition during those years. These peaks likely reflect elevated emissions associated with dry-season accumulation and anthropogenic combustion activities, including industrial operation and biomass burning. In contrast, 2021 showed generally lower concentrations for most ions, coinciding with wetter conditions influenced by a strong La Niña event, which may have enhanced washout and dilution effects.

The rainwater pH values mirrored these ionic trends, with the lowest medians observed in 2020 and 2022, indicating more acidic conditions. Notably, even in the relatively wetter years, the median pH often remained close to or below the critical threshold of 5.6, reaffirming the persistent acidification risk.

Ammonium (NH_4^+) concentrations showed a marked increase in 2023, possibly due to post-pandemic recovery in fertilizer use and agricultural intensity. Meanwhile, chloride (Cl^-) exhibited less consistent variation, although a tendency toward higher values in later years may indicate increasing emissions from urban and coastal sources.

Cumulative rainfall (CH) did not exhibit a unidirectional trend across the five years, emphasizing that changes in ionic concentrations are not solely governed by precipitation amount but also by emission intensity and timing.

Taken together, these interannual patterns underscore the importance of long-term, high-resolution monitoring to detect emerging trends and policy-relevant changes in atmospheric deposition. They also reveal that even in high-rainfall tropical environments, deposition chemistry remains sensitive to anthropogenic and climatic drivers.

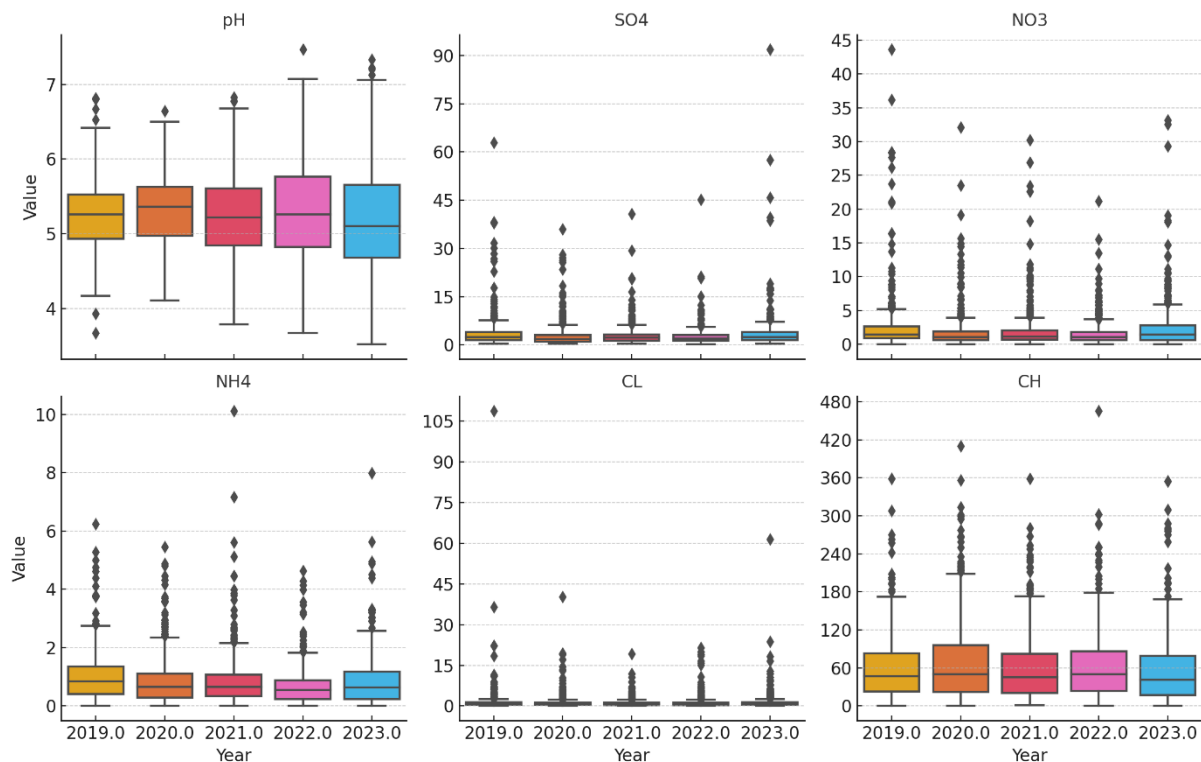


Figure 8. Annual boxplots (2019–2023) of weekly rainwater parameters across Java Island: pH, sulfate (SO_4^{2-}), nitrate (NO_3^-), ammonium (NH_4^+), chloride (Cl^-), and cumulative rainfall (CH). Each box represents the interquartile range (IQR), with horizontal lines indicating the median, and whiskers showing data dispersion. Outliers are plotted individually. Data are aggregated from all thirteen monitoring stations.

Synthesis and Implications. This study provides a comprehensive account of the spatial, temporal, and process-driven variability of rainwater chemistry across Java Island, Indonesia, over a five-year period. Through the integration of descriptive analysis, spatial mapping, mechanistic interpretation, mixed-effects modeling, and seasonal disaggregation, the research reveals a chemically heterogeneous wet deposition regime influenced by urbanization, agricultural intensification, meteorological dynamics, and emission cycles. Notably, acidifying ions, sulfate and nitrate, consistently dominate the ionic profile, with levels frequently surpassing ecological risk thresholds. These conditions are compounded by ammonium-driven buffering that is both spatially uneven and seasonally constrained.

What emerges is a rainwater chemistry regime shaped not solely by meteorology but by a confluence of anthropogenic forces and monsoonal timing. Dry-season accumulation of pollutants, followed by their episodic release during early rainfall events, produces intensified deposition episodes. The nonlinearity between rainfall volume and ionic concentrations, particularly in transition seasons, highlights the limitations of relying on precipitation as a simple cleansing mechanism. This nuance is especially critical in tropical monsoon regions, where rainfall events coincide with shifts in emission regimes and atmospheric mixing depths.

In a broader Southeast Asian context, these findings challenge the assumption that acid rain is predominantly a temperate phenomenon. Despite high rainfall volumes, Java exhibits deposition frequencies and acid rain characteristics comparable to industrialized regions in East Asia, as evidenced by the 47% exceedance rate of the pH 5.6 threshold. This suggests that rainwater in equatorial urban corridors is increasingly burdened by combustion-related acid precursors, with insufficient natural buffering. Without policy intervention, this trend could exacerbate soil acidification, nutrient imbalance, and ecosystem vulnerability, especially in high-density agricultural zones where acid and nitrogen deposition intersect.

The results underscore the urgent need for Indonesia to institutionalize atmospheric deposition monitoring, integrating it with air quality and ecosystem health frameworks. Moreover, these findings support calls for stronger regional cooperation under ASEAN environmental protocols, particularly concerning sulfur and nitrogen management. Future research should expand the spatial domain to encompass eastern Indonesia and link deposition patterns with soil chemistry and crop productivity. Developing predictive models for acid deposition hotspots and evaluating the efficacy of emission control measures would further enhance policy relevance. Additionally, selecting monitoring sites located near major local emission sources—such as power plants,

industrial zones, and biomass burning areas—could help identify source-specific signatures and better understand the episodic nature of acidifying deposition.

4. Conclusion

This study quantitatively assessed the dynamics of wet deposition and rainwater chemistry across Java Island, Indonesia, using high-frequency event-based measurements and mixed-effects modelling. On average, rainwater pH across stations ranged from 5.1 to 6.5, with more than 30% of weekly events exhibiting pH values below the critical threshold of 5.6. Elevated concentrations of sulfate ($\text{SO}_4^{2-} > 5$ mg/L) and nitrate ($\text{NO}_3^- > 2$ mg/L) were also recorded in several urban stations, indicating heightened risk of acid deposition, particularly during the dry season when dilution from rainfall is limited. These findings confirm the dominant role of precipitation in cleansing acidic ions from the atmosphere, while also revealing spatial inequalities in exposure, with urban and industrial zones experiencing the most severe chemical loads. The results provide new empirical support for wet scavenging mechanisms in tropical monsoon systems and underscore the need to strengthen emission control efforts. Future research should incorporate aerosol speciation and targeted monitoring near emission sources to further enhance policy relevance and spatial diagnostics of atmospheric deposition.

Suggestion

Based on the findings of this study, several recommendations can be proposed for future research and policy development:

- 1) Institutionalizing Wet Deposition Monitoring in Indonesia: There is an urgent need to institutionalize rainwater chemistry monitoring within Indonesia's environmental regulatory framework. Existing air quality policies neglect wet deposition, despite its demonstrated ecological relevance. Routine event-based sampling across urban, peri-urban, and agricultural zones should be prioritized.
- 2) Integrating Acid Deposition Thresholds into Environmental Policy: National environmental standards should adopt internationally recognized thresholds for rainwater pH, sulfate, and nitrate concentrations (e.g., WHO, Galloway et al.), to support early warning systems for acid deposition and its ecological risks.
- 3) Expanding Spatial Coverage and Network Density: Future monitoring efforts should include underrepresented regions in eastern Indonesia and integrate coastal–inland transects to capture broader gradients of deposition influenced by maritime and continental air masses.

- 4) Linking Deposition Data with Ecosystem Impact Studies: Observed exceedances in ion concentrations call for integrated assessments of soil acidification, vegetation stress, and aquatic impacts. Linking rainwater chemistry with ecological response indicators will strengthen environmental risk evaluation.
- 5) Promoting Cross-Disciplinary Research and Climate Modeling: Given the demonstrated role of monsoonal dynamics, future studies should couple atmospheric chemistry data with high-resolution meteorological and climate models to better predict spatiotemporal variability in deposition under climate change scenarios.

Acknowledgement

The authors would like to express their sincere gratitude to the Meteorological, Climatological, and Geophysical Agency (BMKG) of Indonesia for providing the comprehensive datasets used in this study, including both meteorological observations and rainwater chemistry analyses. Appreciation is also extended to all field personnel and laboratory teams involved in the data collection and chemical measurement processes across the monitoring stations. The constructive feedback from anonymous reviewers is gratefully acknowledged, as it significantly improved the quality of this manuscript. This research received no specific grant from any funding agency in the public, commercial, or not-for-profit sectors.

References

- [1][1] T. K. Westberry, M. J. Behrenfeld, Y. Shi, H. Yu, L. A. Remer, and H. Bian, "Atmospheric Nourishment of Global Ocean Ecosystems," *Science* (80-.), 2023, doi: 10.1126/science.abq5252.
- [2] M. Peacock *et al.*, "Three Decades of Changing Nutrient Stoichiometry From Source to Sea on the Swedish West Coast," *Ecosystems*, 2022, doi: 10.1007/s10021-022-00798-x.
- [3] C. Chen, W. Xiao, and H. Y. H. Chen, "Mapping Global Soil Acidification Under N Deposition," *Glob. Chang. Biol.*, 2023, doi: 10.1111/gcb.16813.
- [4] X. Liu *et al.*, "Environmental Impacts of Nitrogen Emissions in China and the Role of Policies in Emission Reduction," *Philos. Trans. R. Soc. a Math. Phys. Eng. Sci.*, 2020, doi: 10.1098/rsta.2019.0324.
- [5] L. Du, L. Tang, X. Zheng, and Y. Li, "A Global Analysis of Plant Nutrient Limitation Affected by Atmospheric Nitrogen and Phosphorous Deposition," *Front. Plant Sci.*, 2024, doi: 10.3389/fpls.2024.1473493.
- [6] A. Kalvāns *et al.*, "Nitrate Vulnerability of Karst Aquifers and Associated Groundwater-

- Dependent Ecosystems in the Baltic Region,” *Environ. Earth Sci.*, 2021, doi: 10.1007/s12665-021-09918-7.
- [7] A. Marszałek, K. Affek, M. Załęska-Radziwiłł, and M. Dudziak, “Integrated Ozonation and Photocatalysis to Remove Pollutants for Reuse of Rainwater,” *Sustainability*, 2024, doi: 10.3390/su16135352.
- [8] I. U. Iroegbulem, U. U. Egereonu, C. E. Ogukwe, J. C. Egereonu, N. J. Okoro, and C. I. A. Nwoko, “Assessment of Heavy Metals in Rainwater From Metropolis and Suburbs, Lagos State, Nigeria,” *Int. J. Environ. Clim. Chang.*, 2023, doi: 10.9734/ijeccc/2023/v13i92304.
- [9] M. L. Kassamba-Diaby *et al.*, “The Chemical Characteristics of Rainwater and Wet Atmospheric Deposition Fluxes at Two Urban Sites and One Rural Site in Côte D’Ivoire,” *Atmosphere (Basel)*, 2023, doi: 10.3390/atmos14050809.
- [10] F. Brugnone *et al.*, “Atmospheric Deposition Around the Industrial Areas of Milazzo and Priolo Gargallo (Sicily–Italy)—Part A: Major Ions,” *Int. J. Environ. Res. Public Health*, 2023, doi: 10.3390/ijerph20053898.
- [11] Y. Xu, X. Dong, H. Xiao, C. He, and D. Wu, “Water-Insoluble Components in Rainwater in Suburban Guiyang, Southwestern China: A Potential Contributor to Dissolved Organic Carbon,” *J. Geophys. Res. Atmos.*, 2022, doi: 10.1029/2022jd037721.
- [12] J.-S. Swartz *et al.*, “Wet Season Chemical Composition of Atmospheric Wet Deposition at Cape Point,” *Clean Air J.*, 2022, doi: 10.17159/caj/2022/32/1.12866.
- [13] A. Al-Charideh and S. Nasser, “Chemical Composition of Rainwater and the Acid Neutralization Effect at Tartous and Kadmos Sites in Coastal Area of Syria,” 2022, doi: 10.21203/rs.3.rs-2107624/v1.
- [14] L. Kok *et al.*, “Chemical Composition of Rain at a Regional Site on the South African Highveld,” *Water Sa*, 2021, doi: 10.17159/wsa/2021.v47.i3.11861.
- [15] F. Oduber *et al.*, “Chemical Composition of Rainwater Under Two Events of Aerosol Transport: A Saharan Dust Outbreak and Wildfires,” *Sci. Total Environ.*, 2020, doi: 10.1016/j.scitotenv.2020.139202.
- [16] W. Wang, L. Guan, J. Zhao, Z. Sha, and J. Fang, “Chemical Compositions of Rainfall Water in Nyingchi City, Tibet,” *Atmosphere (Basel)*, 2022, doi: 10.3390/atmos13071021.
- [17] C. N. Pham, R. Gorbunov, V. A. Lapchenko, T. Gorbunova, and V. Tabunshchik, “Macro-And Microelements and the Impact of Sub-Mediterranean Downy Oak Forest Communities on Their Composition in Rainwater,” *Forests*, 2024, doi: 10.3390/f15040612.
- [18] R. Vet *et al.*, “A global assessment of precipitation chemistry and deposition of sulfur, nitrogen, sea salt, base cations, organic acids, acidity and pH, and phosphorus,” *Atmos. Environ.*, vol. 93, pp. 3–100, 2014, doi: <https://doi.org/10.1016/j.atmosenv.2013.10.060>.
- [19] A. Mulsandi, Y. Koesmaryono, R. Hidayat, A. Faqih, and A. Sopaheluwakan, “Detecting Indonesian Monsoon Signals and Related Features Using Space–Time Singular Value Decomposition (SVD),” *Atmosphere*, vol. 15, no. 2, 2024, doi: 10.3390/atmos15020187.
- [20] A. Mulsandi, Y. Koesmaryono, R. Hidayat, A. Faqih, and A. Sopaheluwakan, “On The Interannual Variability of Indonesian Monsoon Rainfall (IMR): A Literature Review of The Role of its External Forcing,” *J. Meteorol. dan Geofis.*, vol. 24, no. 2 SE-Article, pp. 115–127, Mar. 2024, doi: 10.31172/jmg.v24i2.1049.
- [21] A. Löhr *et al.*, “Natural Pollution Caused by the Extremely Acid Crater Lake Kawah Ijen, East Java, Indonesia (7 pp),” *Environ. Sci. Pollut. Res.*, vol. 12, no. 2, pp. 89–95, 2005, doi: 10.1065/espr2004.09.118.
- [22] A. Indrawati *et al.*, “Spatiotemporal distribution in chemical composition of wet atmospheric deposition in Bandung Indonesia,” *Environ. Sci. Pollut. Res.*, vol. 31, no. 55, pp. 64295–64313, 2024, doi: 10.1007/s11356-024-35485-y.
- [23] A. M. Aulia, U. N. C. Safitri, and H. Hwihanus, “The Impact of Carbon Emission Disclosure on Firm Value,” *J. Environ. Econ. Sustain.*, vol. 1, no. 3, pp. 1–6, 2024, doi: 10.47134/jees.v1i3.354.
- [24] F. Paulot and D. J. Jacob, “Hidden cost of U.S. agricultural exports: particulate matter from ammonia emissions,” *Environ. Sci. Technol.*, vol. 48, no. 2, pp. 903–908, Jan. 2014, doi: 10.1021/es4034793.
- [25] J. L. Collett, P. Herckes, S. Youngster, and T. Lee, “Processing of atmospheric organic matter by California radiation fogs,” *Atmos. Res.*, vol. 87, no. 3, pp. 232–241, 2008, doi: <https://doi.org/10.1016/j.atmosres.2007.11.005>.
- [26] X. L. Pan *et al.*, “Estimation of lifetime of carbonaceous aerosol from open crop residue burning during Mount Tai Experiment 2006 (MTX2006),” *Atmos. Chem. Phys. Discuss.*, vol. 12, pp. 14363–14392, 2012, doi: 10.5194/acpd-12-14363-2012.

- [27] J. M. Moch *et al.*, “Global Importance of Hydroxymethanesulfonate in Ambient Particulate Matter: Implications for Air Quality,” *J. Geophys. Res. Atmos.*, vol. 125, no. 18, p. e2020JD032706, 2020, doi: <https://doi.org/10.1029/2020JD032706>.
- [28] M. Pardede *et al.*, “Perspectives of Sustainable Development vs. Law Enforcement on Damage, Pollution and Environmental Conservation Management in Indonesia,” *J. Water Clim. Chang.*, vol. 14, no. 10, pp. 3770–3790, 2023, doi: 10.2166/wcc.2023.417.
- [29] N. Ulibarrí, M. T. Imperial, S. Siddiki, and H. Henderson, “Drivers and Dynamics of Collaborative Governance in Environmental Management,” *Environ. Manage.*, vol. 71, no. 3, pp. 495–504, 2023, doi: 10.1007/s00267-022-01769-7.
- [30] A. Maryono *et al.*, “Study of Individual and Communal Type Rainwater Harvesting Designs, (Case Study: Sawojajar Village, Wanasari District, Brebes Regency, Central Java),” *Media Komun. Tek. Sipil*, vol. 29, no. 2, pp. 261–270, 2024, doi: 10.14710/mkts.v29i2.58284.
- [31] M. F. S. Kartika, M. P. Ningsih, M. A. D. Saputra, S. S. A. A. L. Fq, F. F. Hadianta, and M. H. H. Ichsan, “Rain Harvester Prototype Integration for Drinking Water Using IoT and Mobile Apps,” *J. Inf. Technol. Comput. Sci.*, vol. 8, no. 1, pp. 41–51, 2023, doi: 10.25126/jitecs.202381452.
- [32] K. Khayan, A. H. Husodo, I. Astuti, S. Sudarmadji, and T. S. Djohan, “Rainwater as a Source of Drinking Water: Health Impacts and Rainwater Treatment,” *J. Environ. Public Health*, vol. 2019, pp. 1–10, 2019, doi: 10.1155/2019/1760950.
- [33] S. N. Sakati *et al.*, “Utilization of Rainwater as Consumable Water With Rainwater Harvesting Methods: A Literature Review,” *Pharmacogn. J.*, vol. 15, no. 6s, pp. 1254–1257, 2024, doi: 10.5530/pj.2023.15.227.
- [34] N. Nawan, H. Priskila, H. E. Shinta, S. Handayani, and R. Abdurahman, “Quality of the Peat Water and Its Association With Public Health Problems in the Community of the Danau Tundai Area,” *J. Kedokt. Dan Kesehat. Indones.*, pp. 163–171, 2023, doi: 10.20885/jkki.vol14.iss2.art7.
- [35] M. Hidayat, A. Ikhsano, A. H. Assegaf, and R. S. Fauzan, “Community-Based Disaster Mitigation Communication Strategy Through Rainwater Harvesting Movement,” *Int. J. Prof. Bus. Rev.*, vol. 8, no. 8, p. e01641, 2023, doi: 10.26668/businessreview/2023.v8i8.1641
- [36] P. Pranyoto, M. R. L. Ekowanti, S. Soenyono, and E. Suhardono, “Multilevel Environmental Governance in Indonesia: Analysis of Implementation Pathways and Institutional Dynamics,” *Int. J. Multidiscip. Res. Anal.*, vol. 07, no. 10, 2024, doi: 10.47191/ijmra/v7-i10-46.
- [37] L. Yustitianiingtyas, L. Pratiwi, A. Irawan, D. Stansyah, and S. Arifin, “Environmental Law Policy in Indonesia: Challenges and Sustainable Justice,” *Iop Conf. Ser. Earth Environ. Sci.*, vol. 1473, no. 1, p. 12046, 2025, doi: 10.1088/1755-1315/1473/1/012046.
- [38] P. Luo *et al.*, “Water Quality Trend Assessment in Jakarta: A Rapidly Growing Asian Megacity,” *PLoS One*, vol. 14, no. 7, p. e0219009, 2019, doi: 10.1371/journal.pone.0219009.
- [39] J. N. Galloway, W. H. Schlesinger, H. Levy II, A. Michaels, and J. L. Schnoor, “Nitrogen fixation: Anthropogenic enhancement-environmental response,” *Global Biogeochem. Cycles*, vol. 9, no. 2, pp. 235–252, 1995, doi: <https://doi.org/10.1029/95GB00158>.
- [40] WHO, *Guidelines for drinking-water quality, 4th edition, incorporating the 1st addendum*, 4th ed. Switzerland: WHO Library Cataloguing-in-Publication Data, 2017.
- [41] J. C. Pinheiro and D. M. Bates, *Mixed-Effects Models in S and S-PLUS*, 1st ed. New York: Springer New York, NY, 2000.
- [42] P. Schober and L. A. Schwarte, “Correlation coefficients: Appropriate use and interpretation,” *Anesth. Analg.*, vol. 126, no. 5, pp. 1763–1768, May 2018, doi: 10.1213/ANE.0000000000002864.
- [43] J. H. Einfeld and S. N. Pandis, *Atmospheric Chemistry and Physics: From Air Pollution to Climate Change*, 3th ed. New York: Hoboken, N.J.: Wiley, c2016., 2016.
- [44] C. Giri, “Mapping and Monitoring of Mangrove Forests of the World Using Remote Sensing,” in *A Blue Carbon Primer*, 1st Editio., 2018, p. 15.
- [45] C. Galy-Lacaux *et al.*, “Gaseous emissions and oxygen consumption in hydroelectric dams: A case study in French Guyana,” *Global Biogeochem. Cycles*, vol. 11, no. 4, pp. 471–483, 1997, doi: <https://doi.org/10.1029/97GB01625>.
- [46] S. N. Behera, M. Sharma, V. P. Aneja, and R. Balasubramanian, “Ammonia in the atmosphere: a review on emission sources, atmospheric chemistry and deposition on terrestrial bodies,” *Environ. Sci. Pollut. Res.*, vol. 20, no. 11, pp. 8092–8131, 2013, doi: 10.1007/s11356-013-2051-9.

- [47] Y. Zhang *et al.*, “Aerosol chemistry and particle growth events at an urban downwind site in North China Plain,” *Atmos. Chem. Phys.*, vol. 18, no. 19, pp. 14637–14651, 2018, doi: 10.5194/acp-18-14637-2018.
- [48] C. Perrino, M. Catrambone, A. Di Menno Di Bucchianico, and I. Allegrini, “Gaseous ammonia in the urban area of Rome, Italy, and its relationship with traffic emissions,” *Atmos. Environ.*, vol. 36, pp. 5385–5394, 2002.
- [49] J. Lelieveld *et al.*, “Global Air Pollution Crossroads over the Mediterranean,” *Science* (80-), vol. 298, no. 5594, pp. 794–799, Oct. 2002, doi: 10.1126/SCIENCE.1075457.
- [50] D. G. Streets *et al.*, “An inventory of gaseous and primary aerosol emissions in Asia in the year 2000,” *J. Geophys. Res. Atmos.*, vol. 108, no. D21, 2003, doi: <https://doi.org/10.1029/2002JD003093>.
- [51] M. Wang, M. Wu, and H. Huo, “Life-cycle energy and greenhouse gas emission impacts of different corn ethanol planttypes,” *Environ. Res. Lett.*, vol. 2, no. 2, p. 024001, May 2007, doi: 10.1088/1748-9326/2/2/024001.